INTERNATIONAL JOURNAL OF OPTIMIZATION IN CIVIL ENGINEERING
Int. J. Optim. Civil Eng., 2013; 3(2):289-312

A PRACTICAL WEIGHT OPTIMIZATION FOR MOMENT FRAMES UNDER COMBINED LOADING

M. Grigorian[*,†,a] and A. Kaveh[b]
[a]*MGA, Structural Engineering Inc. 111 N. Jackson St. Glendale, CA.91206, USA*
[b]*Centre of Excellence for Fundamental Studies in Structural Engineering, Iran University of Science and Technology, Tehran-16, Iran*

ABSTRACT

This article introduces three simple ideas that lead to the efficient design of regular moment frames. The finite module concept assumes that the moment frame may be construed as being composed of predesigned, imaginary rectangular modules that fit into the bays of the structure. Plastic design analysis aims at minimizing the demand-capacity ratios of elements of ductile moment frames by inducing the strength and stiffnesses of groups of members in accordance with certain design criteria, rather than investigating their suitability against the same rules of compliance. Collapse modes and stability conditions are imposed rather than investigated. In short, theory of structures is applied rather than followed. Plastic displacement control suggests that in addition to conducting failure analysis, the maximum displacements of plausible failure modes at incipient collapse should also be taken into consideration. While two collapse mechanisms may share the same carrying capacity, their maximum displacements may be different.

Received: 18 February 2013; Accepted: 15 April 2013

KEY WORDS: weight optimization, plastic design, modular analysis, lateral displacements, moment frames.

1. INTRODUCTION

The technical benefits of Plastic Design (PD) have been amply documented in the literature

[*]Corresponding author: M. Grigorian, MGA, Structural Engineering Inc. 111 N. Jackson St. Glendale, CA.91206, USA
[†]E-mail address: Markarjan@aol.com (M. Grigorian)

as well as such authoritative texts as [1-4]. PD has been recognized by many jurisdictions, e.g. [5-7] as an effective means of member sizing for ductile structures in general and moment frames in particular. In recent years, there has been a revival of interest in plastic design in connection with earthquake resistant moment frames [8-11]. Pushover analysis, which is a byproduct of PD has been devised to compute the ultimate carrying capacities of ductile structures under lateral loading [12, 13]. It is a powerful means for understanding the nonlinear response of ductile systems due to sequential formations of plastic hinges. As an investigative design tool, it aims at assessing drift ratios at first yield, before plastic failure and or at incipient collapse. Pushover analysis does not aim at controlling the sequence of formation of the plastic hinges nor does it attempt to reduce material consumption. Plastic analysis is also the basis of the contemporary displacement-based seismic design of engineering structures [14-17]. PD has also been recognized as the most reliable means of design against progressive collapse [18-19].

Recently there has been a surge in novel optimization techniques that aim at improved cost and performance of engineering structures, e.g., [20-29]. Optimization techniques that aim at minimizing material weight, seek solutions that not only satisfy the design criteria, but also try to maximize the number of members with demand-capacity ratios as close to unity as possible. The simplest of these solutions are those that mimic structures of uniform response, [30-32], where the demand–capacity ratios of all members are either equal or close to unity. Theoretically speaking, all members of structures of uniform response fail simultaneously at ultimate loading. However, there is no reason why the processes involved in pushover and optimization techniques cannot be reversed by first selecting a preferred collapse mechanism, then working backwards to select members that would lead to an optimized outcome.

The current article introduces Plastic Design Analysis (PDA) as a simple method of design for lateral resisting moment frames with a view towards displacement control and prevention of development of premature plastic hinges anywhere within the structure. PDA is in fact a design oriented interpretation of the classical PD methods of ductile structures. Most importantly, PDA tends to minimize the volume of computations needed to design an efficient moment frame under lateral loading. PDA is a practical design approach, and as such avoids generalities and unnecessary computations, but relies heavily on understanding the theoretical aspects of plastic response. In PDA theory of structures is applied rather than followed. For instance, realizing that displacements at first yield and at incipient collapse are of greater importance than their interim counterparts, the thrust of the effort is directed towards locating the points of formations of the first and last sets of plastic hinges developed within the structure. In PDA, failure patterns, member strengths, drift ratios and loss of stability are not checked again for code compliance. PDA is not a method of analysis. It is however, an analytic tool for producing structure specific designs. The reader is cautioned that, for the sake of clarity, the effects of offset hinging, strain hardening, yield over strength, local instabilities, as well as panel zone, axial and shear strains have been ignored throughout this presentation. The use of the proposed formulae is ideally suited to case specific and preliminary design purposes. Several parametric examples have been provided to illustrate the applications of the proposed solutions.

2. RATIONALE

The algorithm, defining the use of imaginary modules as constitutive elements of moment frames, assumes that that the entire structure including the grade beams, is composed of imaginary, rectangular, rigidly connected modules that fit into the bays of the framework [33]. Consequently, if each minimum weight module is designed in accordance with the prescribed criteria, then the entire assembly could also be regarded as a minimum weight frame that complies with the same design rules. In other words, the design of one such module can be utilized to generate geometrically similar modules in order to reconstruct the prototype. It has been assumed, for the sake of simplicity, that these imaginary modules are first assembled next to each other to model an optimized horizontal sub-frame. Similar sub-frames are then generated and stacked on top of each other to reconstruct the original structure. The rationale leading to the complete design of an optimized multilevel moment frame is presented in three distinct but related stages. The first stage describes the development of a computational template or basic module, such as that shown in Figure 1(g). The second stage discusses the evolution and optimization of the horizontal sub-frames that constitute the completed structure. In the final stage the sub-frames are proportioned with respect to their racking moments and are mounted on top of each other to recreate the original framework.

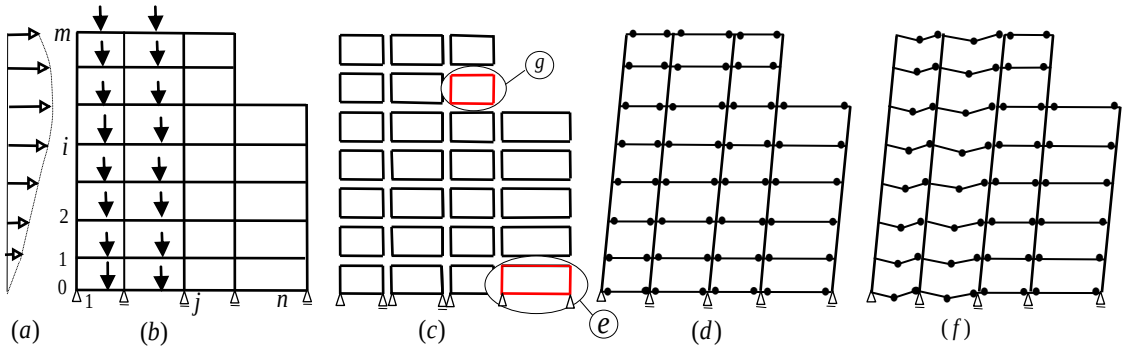

Figure 1. (a) Lateral loading, (b) Regular Moment frame, (c) Constitutive modules, (d) Preferred global sway mechanism, (e) Grade beam supported imaginary module, (f) Combined mechanism, (g) Typical imaginary module

In this approach the basic modules are designed in relation with prescribed loading and target drift ratios. These modules are selected in such a way as to enforce the global collapse mechanisms of figures 1(d) or 1(f) without violating the prescribed drift limits at incipient collapse. The method leads to efficient initial designs rather than analyzing designs that may lead to acceptable preliminary solutions. The proposed methodology involves no complex mathematics or iterative processes.

3. DEVELOPMENT OF BASIC MODULES

The development of the basic module is carried out in two distinct but related steps. Stage

one examines the various collapse modes associated with combinations of constant gravity forces *W* and *P* and a monotonically increasing lateral load *V*. The first stage studies lead to the establishment of permissible load combination regions, such as the quadrangle "abco" of Figure 2. The knowledge that the weak beam-strong column principle precludes the formation of plastic hinges at column ends reduces the number of admissible failure mechanisms to those depicted in figures 2(b) through 2(f). It may be evident that if the module is to withstand relatively large lateral forces, its horizontal members should be strong enough not to fail prematurely as independent beam mechanisms. This hints to the possibility that the sway mode II may be associated with smaller lateral displacements than those corresponding to the combined beam-sway mechanisms III-1, III-2 and III-3. The exclusion of joint mechanisms at column ends immensely facilitates the discussions pertaining to these failure patterns as presented in the prospecting sections. Once the permissible load-interaction region is established, the failure mechanism associated with the largest side sway at incipient collapse can be identified as the more critical failure mode for final design purposes. The more critical failure mode undergoes larger displacements under relatively larger lateral forces. The *critical design* region is indicated by rectangle "cbdo" in Figure 2. Stage two studies involve the derivation of the lateral displacements of the critical failure patterns at incipient collapse. In practical terms, any design fitting within the permissible interaction region would be guarantied to fail through an imposed failure pattern without exceeding the prescribed drift ratios at first yield and at incipient collapse.

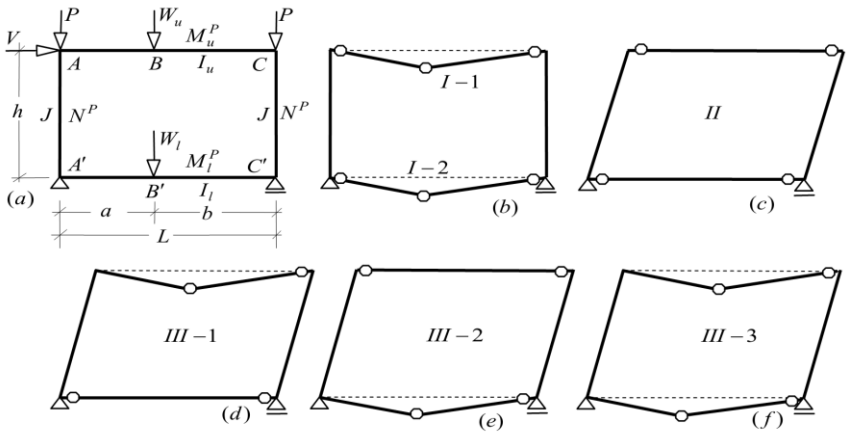

Figure 2. (a) Generalized basic module, (b) Collapse modes I-1 and I-2, (c) Collapse mode II, (d) collapse mode III-1, (e) Collapse mode III-2, (f) Collapse mode III-3

3.1. Step 1: Failure mechanisms

The lateral displacements of a generalized basic module, such as that shown in Figure 2(a), at incipient collapse may be related to mode specific displacement ranges $1 \geq \alpha \geq -1$ and $1 \geq \beta \geq 0$ for sway and combined modes of failure respectively. The auxiliary range functions α and β can then be incorporated as part of the load-resistance interaction diagram to relate the maximum lateral displacements to the corresponding load combination at the onset of plastic collapse. Here, M^P and N^P, and *I* and *J* stand for plastic moments of

resistance and moments of inertias of beams and columns respectively. Suffices *u* and *l* refer to upper and lower levels respectively. *L* and *h* represent the span and the height of the module respectively. *P, W* and *V* are independent, monotonically increasing gravity and lateral forces acting as shown on the module. The six independent load-resistance interaction equations together with their displacement range functions describing the plastic limit states of the generalized basic module of Figure 2(a), may be presented as;

$$\text{Mode I-1:} \quad V = 0, \qquad W_u = \frac{2M_u^P L}{ab} \quad \text{for} \quad \alpha = -1 \tag{1}$$

$$\text{Mode I-2:} \quad V = 0, \qquad W_l = \frac{2M_l^P L}{ab} \quad \text{for} \quad \alpha = -1 \tag{2}$$

$$\text{Mode II: } W_u < \frac{2M_u^P L}{ab} \text{ and } W_l < \frac{2M_l^P L}{ab}, \ \frac{Vh}{f_{cr}} = 2(M_u^P + M_l^P) \ \ \alpha = 1 \text{ and } 0 \geq \beta \geq 1 \tag{3}$$

$$\text{Mode III-1: } W_u \geq \frac{2M_u^P L}{ab} \text{ and } W_l < \frac{2M_l^P L}{ab}, \ \frac{Vh}{f_{cr}} + W_u a = 2\left[M_l^P + \left(\frac{L}{b}\right) M_u^P \right], \ 1 \geq \alpha \geq -1 \tag{4}$$

$$\text{Mode III-2: } W_u < \frac{2M_u^P L}{ab} \text{ and } W_l \geq \frac{2M_l^P L}{ab}, \ \frac{Vh}{f_{cr}} + W_l a = 2\left[M_u^P + \left(\frac{L}{b}\right) M_l^P \right], \ 1 \geq \alpha \geq -1 \tag{5}$$

$$\text{ModeIII-3: } W_u \geq \frac{2M_u^P L}{ab} \text{ and} W_l \geq \frac{2M_l^P L}{ab}, \frac{Vh}{f_{cr}} + (W_u + W_l)a = 2\left[M_u^P + M_l^P\right] \times \left(\frac{L}{b}\right), \ 1 \geq \alpha \geq -1 \tag{6}$$

where, $f_{cr} = 1 - 2P/Kh$ is the load magnifying factor due to racking P-delta effects, [34], and *K* is stiffness of the module at incipient failure. Appropriate values of *K* may be derived from the corresponding displacement equations presented in the next section.

A graphical presentation of group of Eqs.1-6 including their auxiliary displacement ranges is provided in Figure 3. The forthcoming presentation is further simplified, without loss of generality, by introducing the loading ratio $\mu = M_l^P/M_u^P = W_l/W_u$ and the auxiliary range functions $\alpha = M_A/M_u^P$ and/or $\alpha = M_A/M_l^P$, and, $\beta = M_B/M_u^P$ and or $\beta = M_{B'}/M_u^P$ where suffices *A, B, C,* etc., refer to specific locations along the members of the module. It may be evident from group of Eqs.(1) and/or Figure 3 that for $\mu=1$, $M_l^P = M_u^P = M^P$, $W_l = W_u = W$. As a result modes I-1and I-2, and, modes III-1,III-2 and III-3 coincide, in which case points a, b and c coincide with coordinates $W=2M^PL/ab$, $W=M^PL/ab$ and $V=4M^PL/ab$ respectively. Both α and β can be related to the static equilibrium conditions of the beams of the subject module at incipient collapse, i.e.

$$\alpha = \frac{2L}{b} - 1 - \frac{Wa}{M^P} \quad \text{for} \quad \beta = 1 \quad \text{and} \quad \beta = \frac{2b}{L} - 1 + \frac{Wab}{LM^P} \quad \text{for} \quad \alpha = 1 \tag{7}$$

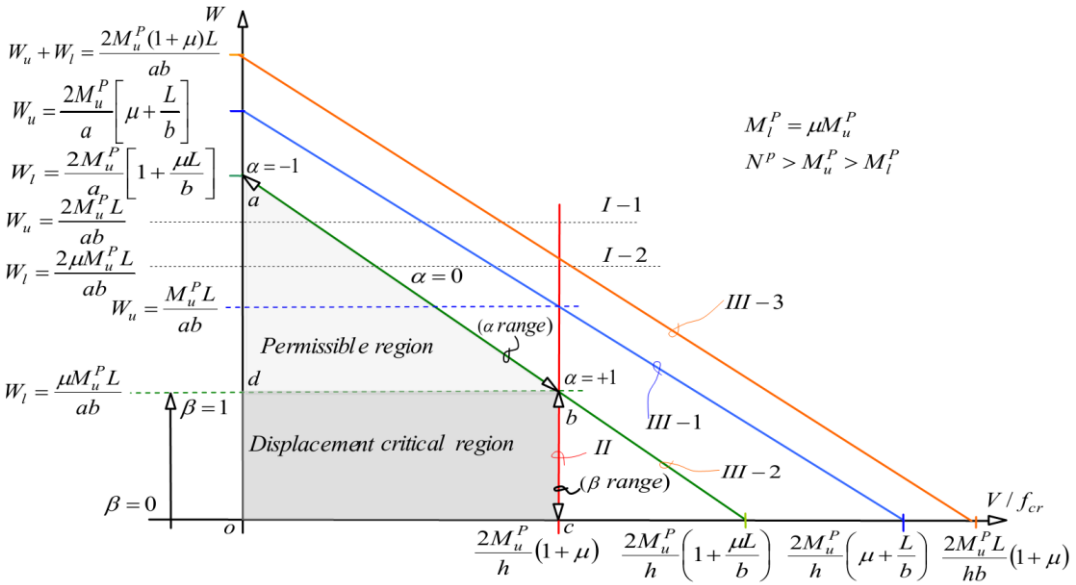

Figure 3. Load-displacement interaction diagram indicating permissible and desirable regions

While the satisfactory vales of M^P with respect to P, V and W are confined to the permissible load-interaction region *oabc*, Figure 3, the more critical selection region is further limited to the rectangle *odbc*, where the module can develop its largest displacement capacity at incipient collapse without violating the prescribed yield criteria. Lines *ab* and *bc* indicate the outer permissible limits of the interactive forces P, W and V corresponding to failure modes III-2and II respectively. They also serve as the auxiliary displacement range indicators α and β of the same failure modes. It may be instructive to note that the maximum ultimate displacement range $1 \le \alpha \le -1$ displayed by line *ab* corresponds to the ultimate lateral force rang $0 \le Vhf_{cr} \le 2M_u^P(1+\mu)$, and that the maximum ultimate displacement range $0 \le \beta \le 1$ displayed by line *bc* corresponds to the ultimate lateral force range $0 \le W_l \le \mu M_u^P L / ab$. Points *a* and *c* represent states of overloading where the module becomes unable to sustain combined forces.

3.2. Step 2-Plastic displacements

Maximum deformations of the module at incipient collapse are associated with the stiffness of the last remaining stable segment of the system that contains the locations of formation of the last set of plastic hinges prior to failure. In other words the accuracy of the computed displacements at incipient collapse depends also on the accuracy of the assumed sequence of formation of plastic hinges throughput the loading history of the structure. In this context, the largest maximum displacements are always associated with the correct positioning of the

last individual or set of plastic hinges. The challenge therefore, is to envisage the patterns and sequences of formation of the plastic hinges during the loading history of the structure, [35-38] etc. An examination of the plastic failure patterns (1b) through (1f), in conjunction with the generalized plastic moment distribution diagram of Figure A1(a), Appendix 1, reveals two dominant sequences of formation of plastic hinges depending on the relative strengths of the two beams and the magnitudes of gravity forces W_u and W_l. For relatively large forces W_u and W_l, i.e., $\beta = 1$ and $1 \geq \alpha \geq -1$, the first and second sets of plastic hinges may form at points B and B', and C and C' respectively. For a definition of the relative magnitudes of W_u and W_l the reader is referred to the interaction diagram, Figure 3, where line *db* and point *b* separate displacement ranges α and β, which in tern correspond to relatively large and small gravity forces respectively. In other words relatively large gravity forces, identified by $W_l > \mu M_u^P L/ab$, are those associated with beam and combined mechanisms, whereas by contrast small gravity forces, $W_l \leq \mu M_u^P L/ab$, can only be associated with sway type mechanisms.

3.2.1 Case 1: Mode III-3, relatively large span loads

For relatively large forces W_u and W_l, i.e., $\beta = 1$ and, $1 \geq \alpha \geq -1$ the first and second sets of plastic hinges may form at points A and A', and, B and B' respectively. The maximum lateral displacements of the generalized computational template/module at incipient collapse in the α range can be expressed as;

$$\delta = \frac{hM_u^P}{12ELf_{cr}}\left[\left(\frac{1+\mu}{J}\right)(\alpha a + b)h + \left(\frac{1}{I_u} + \frac{\mu}{I_l}\right)\left[(2\alpha+1)a^2 + b^2\right]\right] \tag{8}$$

The minimum drift-minimum weight association, [39], for closed loop rectangular frames states that; *the efficient or minimum weight design of the subject module is one involving beams and columns of equal strength and stiffness*. Therefore, putting; $\mu = 1$, $I_u = I_l = I$, $M_u^P = M_l^P = M^P$ and $W_u = W_l = W$ in Eq. (2) gives after rearrangement;

$$\delta = \frac{hM^P}{6ELf_{cr}}\left[(\alpha a + b)\frac{h}{J} + \left[(2\alpha+1)a^2 + b^2\right]\frac{1}{I}\right] \tag{9}$$

The validity of Eq. (2a) may be verified by checking its particular solutions against existing results. For identical upper and lower beams under equal span loads at *a=b=L/2*, Eq. (2b) reduces to the well-known, [40] relationship:

$$\delta = \frac{M^P h^2}{12EJf_{cr}}\left[1 + \frac{1}{\rho}\right](1+\alpha), \quad \text{where} \quad \rho = JL/Ih \tag{10}$$

A derivation of Eq. (8) is presented in Appendix 1. $\alpha = 1$, at point *b* of the interaction diagram represents an ideal combination of M^P, P, *W* and *V* in that it allows the full displacement development potential of the module in association with a combined mechanism such as III-3. However it should be born in mind that point *b* is also associated with sway type mechanism II that exhibits the same ultimate load carrying potential, but as elaborated in the following section, tends to develop larger displacements at collapse.

3.2.2 Case 2: Mode II, relatively small span loads

For relatively small forces W_u and W_l, i.e., $\beta < 1$ and $\alpha = 1$, the first and second sets of plastic hinges may form at points C and C', and A and A' respectively. The maximum lateral displacements of the generalized computational template/module at incipient collapse in the β range can be expressed as:

$$\delta = \frac{h}{12Ef_{cr}}\left\{\frac{h}{J}\left(M_u^P + M_l^P\right) + \left\{b\left[\beta\left(\frac{2b}{L}+1\right)+\left(2+\frac{b}{L}\right)\right]+a\left[(2\beta-1)\frac{b}{L}\right]\right\}\left[\frac{M_u^P}{I_u}+\frac{M_l^P}{I_l}\right]\right\} \quad (11)$$

A derivation of Eq. (11) is presented in Appendix 2. For the particular case of $\mu = 1$ Eq. (11) reduces to:

$$\delta = \delta_C + \delta_B = \frac{2hM^P}{12Ef_{cr}}\left\{\frac{h}{J}+\frac{b}{I}\left\{\left[\beta\left(\frac{2b}{L}+1\right)+\left(2+\frac{b}{L}\right)\right]+\frac{a}{b}\left[(2\beta-1)\frac{b}{L}\right]\right\}\right\} \quad (12)$$

The validity of Eq. (11) may also be verified by checking its particular solutions against existing results. For identical upper and lower beams under equal span loads at *a=b=L/2*, Eq. (12) reduces to the previously established, [41] formula:

$$\delta = \frac{M^P h^2}{6EJf_{cr}}\left[1+\frac{1}{\rho}\left(\frac{3\beta}{2}+1\right)\right] \quad \text{where} \quad \beta = \frac{WL}{4M^P} \quad (13)$$

A derivation of Eq. (13) is presented in Appendix 2. Note that both displacement Eqs. (10) and (13) contain the relative stiffness term ρ. The location of point *b* in Figure 3 is significant, in that both failure mechanisms II and III-2 share the same demand-capacity ratio, $Vhf_{cr}/2M_u^P(1+\mu)$ but result in different maximum displacements at the onset of collapse This implies that care maximum should be exercised in computing the maximum lateral displacements corresponding to point *b* .The auxiliary displacement ranges α and β are associated with the first sets of plastic hinges forming at mid span and right hand ends of the beams of the subject modules respectively. Solutions (10) and (13) also coincide at $\alpha = 1,\ \beta = 0$, for *W*=0 and $Vhf_{cr} = M_u^P(1+\mu)$.

4. GENERATION OF SUB-FRAMES

It has been argued that a regular sub-frame, such as that shown in Figure 4(a) may be construed as being composed of *n sufficiently strong and stiff* closed loop modules, such as those depicted in Figure 4(c). Integers $j = 0, 1, 2\ldots n$, and $i = 0, 1, 2\ldots m$ are non-dimensional coordinates introduced to identify the elements of the structure. A representative sub-frame is one which has been designed to perform in conformity with pre-set target criteria, and as such may be reproduced, in accordance with certain scaling rules to reconstruct all other sub-frames of the frame.

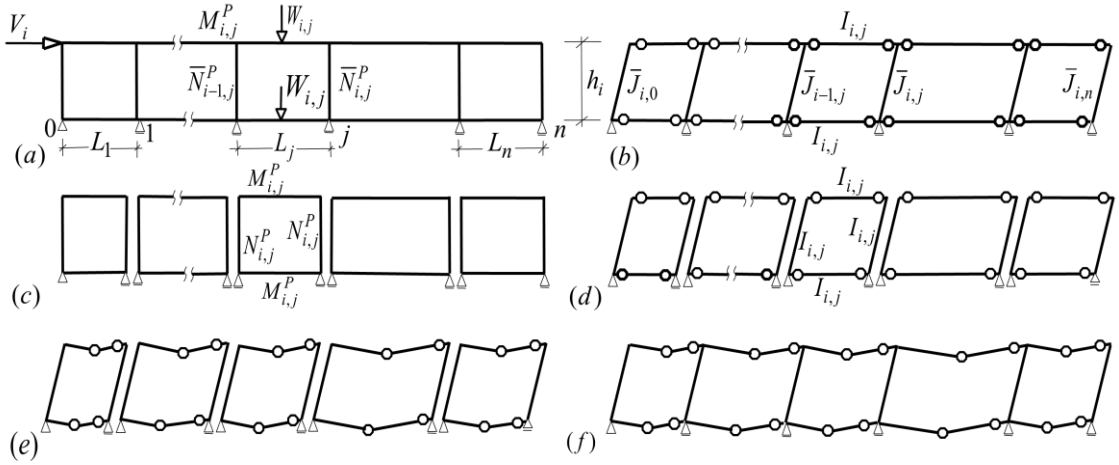

Figure 4. (a) Generalized sub-frame at level *i*, (b) Collapse pattern involving beams only, (c) Basic modules as constituent elements of the sub-frame, (d) Collapse patters corresponding to 3c, (e) Combined collapse patters of individual modules, (f) Combined collapse mechanism of the sub-frame

A properly designed/generated sub-frame should also be capable of distributing the racking reactions to as many supports as possible in a *safe and economic* manner. In order to generate the subject sub-frame without resorting to computers or complicated numerical analysis, recourse has been made to the following axioms and structure specific principles that:

- The sway collapse mode of the prototype, figures 1(d) and 1(f) can be studied through the collapse mechanisms of the corresponding closed loop modules, Figure 4(c).
- Large gravity loads tend to *diminish* the lateral carrying capacity and sway development potentials of closed loop modules. Therefore, beam mechanisms should be disallowed.
- The lateral carrying capacity of the sub-frame can be *assigned* to any one or any number of modules provided that all pertinent rules and conditions are observed.
- If the strength of each module is selected as the minimum strength of its beams when acting as simply supported members, then the entire sub-frame can be expected to fail through a combined or purely sway type mechanism.

- The *first* set of plastic hinges forms at beam ends with the largest demand–capacity ratio. In other words, the first set of plastic hinges tends to form at the stiffer ends of the stiffest module. If there is more than one module with equal maximum stiffness then the first set of plastic hinges will form at the stiffer ends of the weakest beams.
- The maximum displacements at *first yield* are associated with the module containing the *first* set of plastic hinges. Since the maximum allowable drift ratio at first yield, ϕ_Y is associated with the stiffest module, then the minimum stiffness of the stiffest module dominates the elastic performance of the sub-frame.
- The *last* set of plastic hinges form at beam ends with the smallest demand–capacity ratios. In other words, the last set of plastic hinges form at the stiffer ends of the most flexible module. If there is more than one module with equal minimum stiffness then the last set of plastic hinges will tend to form at the more flexible ends of the weakest beams.
- The maximum displacements at *incipient* collapse are associated with the module containing the last set of plastic hinges. Since the maximum allowable drift ratio at collapse, ϕ_P is associated with the most flexible module, then the minimum stiffness of the most flexible module governs the magnitude of the minimum elastic properties of the members of the sub-frame.
- The columns remain *elastic* throughout the history of loading of the structure.

The most *economical* solution using prismatic members is associated with the ultimate strength and elastic properties of the stiffest and the most flexible modules that contain the first and last sets of plastic hinges respectively.

4.1 Minimum module strength for sway mechanism

Consider the plastic design of the sub-frame of Figure 4(a) under the symbolic mid span gravity forces $W_{i,j}$ and upper chord level shear force V_i. To prevent beam type failure the strength of each module may be selected as $M_{i,j}^P \geq \frac{1}{2}(W_{i,j}L_j/4) = W_{i,j}L_j/8$. However, the load resistance interaction diagram of Figure 3 suggests that in order to resist the combined effects of $W_{i,j}$ and V_i , the ultimate strength of each beam of each module can be increased from $M_{i,j}^P$ to $(M_{i,j}^P + \partial M_{i,j}^P)$. In addition the beams of the sub-frame may be strengthened, say by added flange plates or weakened by means of reduced beam sections, [42], to control the sequences of formations of the plastic hinges and/or to fine-tune the performance of the system. The virtual work equations of the sway and the combined mechanisms of figures 4(b) and 4(f), including the effects of the enhancements M can be expressed as:

$$\frac{V_i h}{f_{cr}} = 4\sum_{j=1}^{n}(M_{i,j}^P + \partial M_{i,j}^P) + \mathrm{M} \tag{14}$$

and

$$\frac{V_i h}{f_{cr}} + \sum_{j=1}^{n} W_{i,j}L_j = 8\sum_{j=1}^{n}(M_{i,j}^P + \partial M_{i,j}^P) + \mathrm{M} \tag{15}$$

respectively. Since $\sum_1^n W_{i,j} L_j = 8 \sum_1^n M_{i,j}^P$, Eqs. (14) and (15) can be reduced to:

$$\sum_{j=1}^{n} \partial M_{i,j}^P = \frac{(V_i h / f_{cr}) - \mathrm{M}}{4} - \sum_{j=1}^{n} M_{i,j}^P \tag{16}$$

$$\text{and} \quad \sum_{j=1}^{n} \partial M_{i,j}^P = \frac{(V_i h / f_{cr}) - \mathrm{M}}{8} \tag{17}$$

respectively. The final design of the sub-frame is governed by the more demanding value of Eqs. (16) and (17), which may be used to decide upon the preferred mechanism to resist the force V_i. In other words if, $(V_i h / f_{cr}) > \mathrm{M} + \sum_1^n W_i L_i$ then sway type mechanism will control the ultimate carrying capacity of the structure , otherwise a combined type failure will prevail. Several options for the selection of $\partial M_{i,j}^P$ are available. It would be reasonable, from a purely material consumption point of view, to assign the entire lateral force, or greater portions of it, to the shortest and stiffest/or the shorter and stiffer modules of the frame respectively. For instance, if as option 1, the entire shear force V_i is assigned to the shortest module of the sub-frame of Figure 4, with $L_{short} = L_s$ and $\mathrm{M} = 0$, then the required additional moment of resistance of the selected module and its beams may be computed as $\partial M_{i,s}^P = V_i h / 4 f_{cr}$. Next, assuming that the self-weight of each module, $g_{i,j}$, can be estimated in terms of its own plastic moments of resistance and a constant of proportionality, g, i.e. $g_{i,j} = 2g(h + L_j) M_{i,j}^p$, then the self-weight of the complete sub-frame may be estimated as:

$$G_i = \frac{2g}{8} \left[(h + L_s) \frac{2 V_i h}{f_{cr}} + \sum_{j=1}^{n} (h + L_j) W_{i,j} L_j \right] \tag{18}$$

In practical terms this implies rendering all other modules as ineffective against lateral forces. However, if all modules of the sub-frame are to participate as load resisting elements, then the next best solution may consist of either distributing the lateral force equally between all modules of the sub-frame, in which case the required enhancement would be the larger of the quantities:

$$\partial M_{i,j}^P = \frac{V_i h}{8 n f_{cr}} \quad \text{and} \quad \partial M_{i,j}^P = \frac{V_i h}{4 n f_{cr}} - \frac{1}{n} \sum_{j=1}^{n} M_{i,j}^P \tag{19}$$

or by enhancing the strengths of the individual modules in proportion with their minimum moments of resistance, $M_{i,j}^P = W_{i,j} L_j / 8$ and/or other physical properties. The former choice

gives:

$$G_i = \frac{2g}{8}\left[8\partial M_{i,j}^{P}\sum_{j=1}^{n}(h+L_j)+\sum_{j=1}^{n}(h+L_j)W_{i,j}L_j\right] \tag{20}$$

While option 2, characterized by Eq.(20) indicates a lighter structure than (18) the difference diminishes as L_s approaches $\sum_1^n L_i/n$, and because of constancy of $V_i h$, the two solutions coincide for $L_s = L_i = L$. As a third option consider the proportional enhancement of all loaded beams of the sub-frame as characterized by $\mathrm{M} = 0$ and $\partial M_{i,j}^{P} = \gamma M_{i,j}^{P}$. Eqs. (16) and (17) give the governing value of γ as the greater of:

$$\gamma = \frac{2(V_i h/\ f_{cr} - \mathrm{M})}{\sum_1^n W_{i,j}L_j} - 1 \text{ and } \gamma = \frac{(V_i h/\ f_{cr} - \mathrm{M})}{\sum_1^n W_{i,j}L_j} \tag{21}$$

respectively. The corresponding self-weight may be assessed as:

$$G_i = \frac{2g}{8}\left[\sum_{j=1}^{n}(h+L_j)(1+\gamma)W_{i,j}L_j\right] \tag{22}$$

Eq.(22) indicates a relatively heavier solution than (20). However the two solutions coincide at $L_i = L$. For most practical cases L_i are either equal or nearly equal and the difference between (20) and (22) becomes insignificant. Therefore the stiffer selection option may be better suited for displacement studies.

4.1.1 Demonstrative Example 1

Consider the plastic design of the i^{th} level sub-frame of a four bay (n =4) moment frame with $L_1 = L = h$, $L_2 = 2L$, $L_3 = 3L$ and $L_4 = 4L$, under the combined actions of a lateral shear force $V=10WL$ and mid span gravity forces $W_i = W$, and compare the results of the three member selection strategies described above.

Assume $\mathrm{M} = 0$ and $f_{cr} = 1$.

Solution: Since $(V_i h/\ f_{cr}) = \mathrm{M} + \sum_1^m W_i L_i$ then both sway and combined mechanisms yield the same results. The minimum or base strength of the beams of sub-frame may be computed as $M_{i,1}^{P} = WL/8$, $M_{i,2}^{P} = 2WL/8$, $M_{i,3}^{P} = 3WL/8$ and $M_{i,4}^{P} = 4WL/8$ for all three selection options. The complete solution is presented in Table 1.

It may be observed from the results of Table 1 that all three strategies result in comparable material consumption.

Table 1. Parametric solution, Example 1

Option	$\partial M_{i,j}^{P}$	Eq.	G/gWL^2	Eq.	Shear design strategy
1	$Vh/4$	-	20.00	(18)	By shortest module
2	$Vh/8n$	(19)	18.75	(20)	Equally distributed
3	$M_{i,j}^{P}$	(21)	20.00	(22)	Proportionately distributed

4.2. Minimum module stiffness for sway mechanism

Having established the rules of minimum strength for the preferred design mechanisms, an attempt can now be made to select the properties of the i^{th} level modules in such a way as to satisfy the stipulated target drifts, ϕ_Y at first yield and ϕ_P at incipient collapse. As the second step of the design process, the response of the modules should be related to the corresponding displacement ranges, α or β on the interaction diagram. If the properties of the most flexible and the stiffest modules are identified by suffices *f* and *s* respectively, then using Eq. (10), the corresponding drift ratios for the α range at first yield and incipient collapse may be expressed as:

$$\phi_{Y,i} = \frac{M_{i,s}^{P}}{12EI_{i,s}f_{cr,i}}\left(h+L_s\right) = \frac{M_{i,s}^{P}h}{12EI_{i,s}f_{cr,i}}\left[1+\frac{1}{\rho_{i,s}}\right] = \frac{M_{i,s}^{P}}{h^2 f_{cr}K_{i,s}} \tag{23}$$

$$\text{and, } \phi_{P,i} = \frac{M_{i,f}^{P}(1+\alpha)}{12EI_{i,f}f_{cr,i}}\left(h+L_f\right) = \frac{M_{i,f}^{P}(1+\alpha)h}{12EI_{i,f}f_{cr,i}}\left[1+\frac{1}{\rho_{i,f}}\right] = \frac{M_{i,f}^{P}}{h^2 f_{cr}K_{i,f}} \tag{24}$$

respectively. With $\phi_{Y,i}=\phi_Y$ and $\phi_{P,i}=\phi_P$ known, the plastic to elastic drift ratio of the system may be assessed as $\eta=\phi_P/\phi_Y$. Dividing (23) by (24) and rearranging, gives:

$$\frac{M_{i,s}^{P}}{I_{i,s}} = \frac{(h+L_f)M_{i,f}^{P}}{\eta(h+L_{s)}I_{i,f}} \tag{25}$$

as the characteristic plastic response ratio of the first and last failing modules of the sub-frame, in which case the forces causing first yield and plastic collapse may be computed as:

$$V_{Y,i} = \frac{4M_{i,s}^{P}}{h}\left[\frac{\sum_1^n K_{i,j}}{K_{i,s}}\right] = \frac{4M_{i,s}^{P}}{h}\left[\frac{\sum_1^n k_{i,j}}{k_{i,j}}\right] \tag{26}$$

where $k_{i,j}=I_{i,j}/(h_i+L_j)$ may be regarded as an indication of the relative stiffness of the module. A brief derivation of V_Y is presented in Appendix 3. A similar argument may be

presented for the β range response by using Eq. (13) and following the same steps as Eqs. (23) through (26), in which case the plastic to elastic drift tatio indicator may be expressed as:

$$\frac{M_{i,s}^{P}}{I_{i,s}} = \frac{M_{i,f}^{P}}{\eta I_{i,f}} \left[h + L_f \left(\frac{3\beta_f}{2} + 1 \right) \right] \Big/ \left[h + L_s \left(\frac{3\beta_s}{2} + 1 \right) \right] \tag{27}$$

Once $M_{i,j}^{P}$ and $I_{i,j}$ have been determined for any level *i*, the preliminary design of the original sub-frame can be completed as:

$$J_{i,j} = I_{i,j},\ N_{i,j}^{P} = \lambda M_{i,j}^{P},\ \bar{J}_{i,j} = J_{i,j} + J_{i,j+1} \text{ and } \bar{N}_{i,j}^{P} = N_{i,j}^{P} + N_{i,j+1}^{P} \tag{28}$$

where, $\lambda > 1$ is the code specified column overt strength factor. In addition, the properties of the beams of two adjoining sub-frames may be computed as:

$$\bar{I}_{i,j} = I_{i,j} + J_{i+1,j} \quad \text{and} \quad \bar{M}_{i,j}^{P} = M_{i,j}^{P} + M_{i+1,j}^{P} \tag{29}$$

The purpose of the following example is to demonstrate the applications of the displacement Eqs. (23) and (24) and how to allow for an overloaded module.

4.2.1 Demonstrative Example 2

Design the sub-frame of example 1 for *V*=1423.43 kN, $W_1 = 5V/4,\ W_2 = W_3 = W_4 = 0,$ $\phi_P = 0.0024$ radians, $\eta = 2$, and *E*=199,945 MPa. As a different selection strategy, use uniform sections for the chords of all lateral resisting modules.

Solution: Select $M_{1,\min}^{P} = W_1 L_1 / 8 = 5VL/32$ and $M_2^{P} = M_3^{P} = M_4^{P} = M^{P}$. The inequality $2Vh < W_1 L_1 / 8$, implies that module No.1 is overloaded and as such is unable to contribute to the lateral carrying capacity of the sub-frame. However the three remaining module are capable of resisting the entire external shear force through a partial sway mechanism, i.e. $Vh = 3 \times 4M^{P}$. Since modules 2 and 4 are the stiffest and the most flexible respectively of the remaining modules, then from Eqs. (24) and (25): $I_3 = I_4 = I = 5Vh^2 / 72E\phi_P$ and $I_{2.} = 6I/5$ respectively. Next Eqs.(25) and (26) yield, upon substitution: $K_1 = 0,\ K_2 = 24EI_2/3h^3,\ \sum_1^4 K_i = 102EI/5h^3,\ V_2 = 8V_Y/17,$ $V_Y = 17V/24$ and $V_2 = V/3$ respectively. Consequently Eq. (23) reduces to $\phi_{Y,2} = Vh^3/24EI_2$. The complete preliminary design of the subject sub-frame is presented in Table 2. (The moment of inertia of the none-contributing module No. 1 has been selected arbitrarily as, $I_1 = 2I$).

Table 2. Parametric solution, Example 2

j	M_j^P / M^P	$\bar{N}_j^P / \lambda M^P$	I_j / I	$\bar{J}_j / I$
0	-	15/8	-	2
1	15/8	23/8	2I	3
2	1	2	6/6	2
3	1	2	1	2
4	1	1	1	1

Results of computer analysis as recorded in Table 3, verify the accuracy of the proposed solution. $V_{P,2}$ and $\phi_{P,2}$ are intermediate results describing the failure load and the corresponding lateral displacement of the stiffest module as the strongest component of the example sub-frame.

Table 3. Comparative, PDA/computer results, Example 2

	M^P (kN-m)	V_P (kN)	V_Y (kN)	$V_{P,2}$ (kN)	$\phi_{P,2}$	ϕ_Y	ϕ_P
PDA	361.50	1423.43	1008.26	1008.26	0.00120	0.00120	0.00240
Computer	361.50	1423.43	964.09	998.16	0.00121	0.00118	0.00246

Design solution of example 2, not only satisfies the requirements of the *uniqueness theorem*, [43-44], i.e. mechanism, equilibrium, boundary conditions and the yield criteria but also satisfies the prescribed displacement conditions. And as such, for the given geometry, it cannot be far from a minimum weight product. Nevertheless, several other satisfactory solutions, including $M_1^P = 9VL/8$ and $M_2^P = M_3^P = M_4^P = 0$ can also be suggested.

The purpose of the next example is to demonstrate the applications of the displacement Eqs. (13) and (27), control the sequence of formation of the plastic hinges and how to allow for loading on all modules.

4.2.2 Demonstrative Example 3

Redesign the sub-frame of Figure 4(a) for V=F=569.37 kN, $W_1 = 5W$, $W_2 = 2W$ and $W_3 = W_4 = W = 35.59$ kN. Select the strength and the stiffness of the modules in such a way as to control the sequence of formation of the plastic hinges. s =1, f =4, $\eta_{i,4} = 2$ and $\eta_{i,1} = \eta_{i,2} = \eta_{i,3} = 1.$

Solution: Individual beam mechanisms give $M_1^P = 5WL/8$, $M_2^P = 4WL/8$, $M_3^P = 3WL/8$ and $M_4^P = 4WL/8.$ Doubling the resistance of the beams automatically reduces the demand capacity ratios of the beams to half for vertical loading and increases the lateral carrying capacity of the sub-frame to its permissible maximum $Fh = 4\sum_1^4 2W_j L_j = 2(5+4+3+4)WL/8 = 16WL.$ Since at V=0 and enhanced

moments, $2M_j^P$ the system is still elastic, then the entire sub-frame can respond linearly until the formation of the first set of plastic hinges where the combined demand-capacity ratio is closest to unity. Furthermore, since the increased strengths, $2M_j^P$ are not equal, it would be reasonable to select I_j in proportion to M_j^P, whence substituting $\beta_j = 1$in Eq. (27), it gives:

$$\bar{k}_{i,j} = \frac{I_{i,j}}{(2h+5L_j)}\ ,\ \bar{k}_j = \frac{M_j^P}{M_1^P}\bar{k}_1 \qquad \text{and} \qquad I_{i,j} = \frac{M_{i,j}^P(2h+5L_j)}{\eta_{i,j}M_{i,1}^P(2h+5L_1)}I_{i,1} \tag{30}$$

This gives: $I_1 = 35I/35,\quad I_2 = 48I/35,\quad I_3 = 51I/35,\quad I_4 = 88I/\eta 35,\quad \bar{k}_1 = I/7L,$ $\bar{k}_2 = 4I/35L$, $\bar{k}_3 = 3I/35L,\quad \bar{k}_4 = 4I/35L$ and Consequently $V_{Y,j} = F_Y\bar{k}_j/\sum_1^n\bar{k}_j$ gives: $V_{1,Y} = 35F_Y/178.$ Since the maximum gravity moments at the two right hand corners are still elastic at $M_1^P/2 = 5Wl/8$, then the shear force needed to impose first yield at these locations may be computed as: $F_Y = 5\times 187V/35\times 64$.This in turn gives, $V_{1,Y} = 5V/64,$ $\delta_{1,Y} = \frac{V_{1,Y}h^3}{24EJ_1}\left[1+\frac{1}{\rho_1}\left(\frac{3\beta_1}{2}+1\right)\right] = \frac{35Fh^3}{3072EI_1}$, $\delta_{1,P} = \frac{7M_1^Ph^2}{12EI_1}$ and $\delta_P = \frac{11M_4^Ph^2}{6EI_4}$.

Once again, as indicated in Table 4, there is excellent agreement between manually computed and machine generated results.

Table 4. Comparative, PDA/computer results, Example 3 $I_1 = 719.257\times 10^6\, mm^4$

	M^P (kN-m)	V_P (kN)	V_Y (kN)	$V_{P,1}$ (kN)	$\phi_{P,1}$	ϕ_Y	ϕ_P
PDA	135.58	569.37	237.66	444.82	0.00169	0.0004	0.00336
Computer	135.58	569.37	234.58	519.82	0.00172	0.0004	0.00338

4.3. Proportioning and regeneration of the multi-story moment frame

The individual modules of the i^{th} level imaginary sub-frame of Figure 4 were selected in such a way as to share the same drift ratios at first yield and incipient collapse while remaining in equilibrium with external racking shear force and moment of the same level during both phases of loading. It follows, therefore, that if all other sub-frames of the structure are designed in a similar fashion for the same initial and final drift ratios, then the properties of the individual members can be determined through direct proportioning. For instance, if the m^{th} level members are known then for constant drift $\phi_m = \phi_i$, the i^{th} level member properties may be proportioned as:

$$J_{i,j} = \left[\frac{M_{i,j}^P}{M_{m,j}^P}\right]\left[\frac{h_i}{h_m}\right]\left[\frac{f_{cr,m}}{f_{cr,i}}\right]J_{m,j} = \left[\frac{V_ih_i^2}{V_mh_m^2}\right]\left[\frac{f_{cr,m}}{f_{cr,i}}\right]J_{m,j} \tag{31}$$

$$I_{i,j}=\left[\frac{M^{P}_{i,j}}{M^{P}_{m,j}}\right]\left[\frac{f_{cr,m}}{f_{cr,i}}\right]\left[\frac{3\beta_{i,j}+2}{3\beta_{m,j}+2}\right]I_{m,j}=\left[\frac{V_i h_i}{V_m h_m}\right]\left[\frac{f_{cr,m}}{f_{cr,i}}\right]\left[\frac{3\beta_{i,j}+2}{3\beta_{m,j}+2}\right]I_{m,j} \qquad (32)$$

The fraction $f_{cr,m}/f_{cr,i}$ is generally very close to unity and may be equated to 1 for all practical purposes. Applications of Eqs.(31) and (32) may best demonstrated by the following simple examples.

4.3.1 Demonstrative Example 4

Provide a preliminary efficient design for the four story, grade beam supported moment frame of Figure 5 subjected to the lateral forces: $F_i = Fi/m$, and drift limitations $\phi_{i,Y}=.0017$ radians and $\phi_{i,P}=.0034$ radians. Assume $f_{cr,i,j}=1$ and that example 3 describes the response of the roof level sub-frame of the structure.

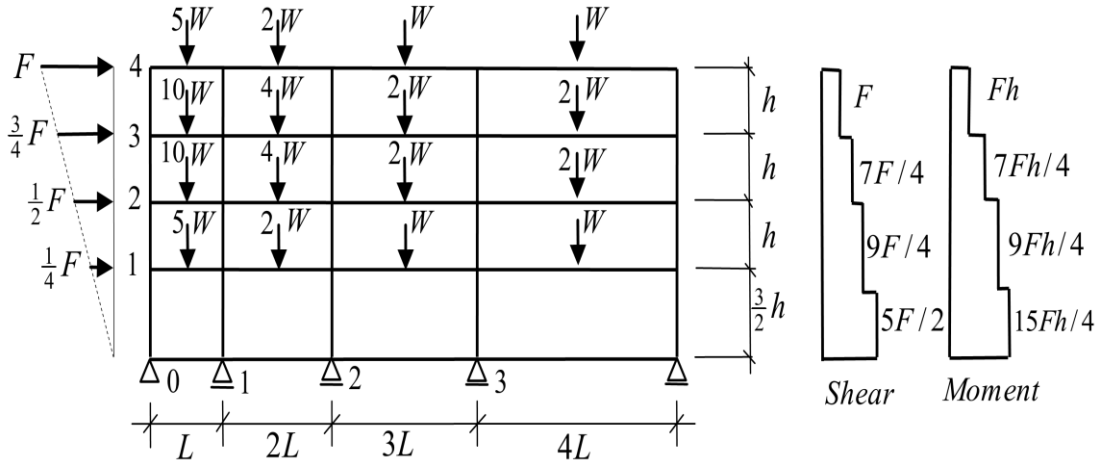

Figure 5. Four story moment frame. Loading, layout, Shear and racking moment diagrams

Solution: The moments of resistance of the roof level modules may be summarized in Table 5 as: $M^{P}_{4,1}=5WL/4=5M^{P}/4$, $M^{P}_{4,2}=4WL/4=M^{P}$, $M^{P}_{4,3}=3WL/4=3M^{P}/4$ and $M^{P}_{4,4}=4WL/4=M^{P}$.

Similarly, the moments of inertias of the same modules may be registered as: $I_{4,1}=J_{4,1}=35I/35$, $I_{4,2}=J_{4,2}=48I/35$, $I_{4,3}=J_{4,3}=51I/35$ and $I_{4,4}=J_{4,4}=44I/35$. Next, the racking moments of the 1st,2nd and 3rd level sub-frames may be rewritten in terms of the roof level moments $M_4=M$ as: $M_1=15M/4$, $M_2=9M/4$ and $M_3=7M/4$, respectively.

Table 5. Summary, design of modules of Example 4*

		j=1			j=2		
i	β	M^P	I	J/I	M^P	I	J/I
4	1.00	1.25	1.00	1.00	1.00	1.37	1.37
3	0.57	2.19	1.30	1.75	1.75	1.78	2.40
2	0.44	2.81	1.50	2.25	2.25	2.06	3.08
1	0.00	4.69	1.50	3.75	3.75	2.06	5.14

		j=3			j=4		
i	β	M^P	I	J/I	M^P	I	J/I
4	1.00	0.75	1.46	1.46	1.00	1.26	1.26
3	0.57	1.32	1.90	2.56	1.75	1.63	2.21
2	0.44	1.69	2.19	3.29	2.25	1.89	2.84
1	0.00	2.81	2.19	5.48	3.75	1.89	4.73

Eqs. (28) and (29) may now be used to complete the preliminary efficient design of the subject frame as summarized in Table 6.

Table 6. Summary, design of 4 story of Example 4*

	j=0		j=1				j=2			
i	$\overline{M}^P$	$\bar{J}$	$\overline{M}^P$	$\overline{N}^P$	$\bar{I}$	$\bar{J}$	$\overline{M}^P$	$\overline{N}^P$	$\bar{I}$	$\bar{J}$
4	1.25	1.00	1.25	2.25	1.00	1.00	1.00	1.75	1.37	1.37
3	3.44	2.30	3.44	3.94	2.30	1.75	2.75	3.07	3.15	2.40
2	5.00	2.80	5.00	5.06	2.80	2.25	4.00	3.94	4.03	3.08
1	7.50	3.00	7.50	8.44	3.00	3.75	6.00	6.56	4.12	5.14
0	4.69	1.50	4.69	-	1.50	-	3.75	-	2.06	-

	j=3				j=4			
i	$\overline{M}^P$	$\overline{N}^P$	$\bar{I}$	$\bar{J}$	$\overline{M}^P$	$\overline{N}^P$	$\bar{I}$	$\bar{J}$
4	0.75	1.75	1.46	1.46	1.00	1.00	1.26	1.26
3	2.07	3.07	3.36	2.56	2.75	2.75	2.89	2.21
2	3.01	3.94	4.09	3.29	4.00	2.25	3.52	2.84
1	4.50	6.56	4.38	5.48	6.00	3.75	3.78	4.73
0	2.81	-	2.19	-	3.75	-	1.89	-

* $\overline{M}^P$ and $\overline{N}^P$, and, $\bar{I}$ and $\bar{J}$ have been summarized as multiples of M^P and I respectively.

5. CONCLUSIONS

This article has introduced three simple ideas that lead to efficient design of regular moment frames-the *finite module* concept, the *Plastic design analysis* and a method of *Plastic displacement control.*

An analytic procedure has been provided to facilitate and revive interest in plastic design of efficient moment frames. The philosophical differences between PDA and PAD have been discussed and demonstrated through generic and numerical examples. In PDA collapse modes and stability conditions are imposed rather than investigated. The theory of structures is applied rather than followed.

Several numerical solutions have been presented to demonstrate the accuracy and applications of the proposed concepts and design formulae.

In upholding the tradition, [45, 46] it has been shown, contrary to the common belief, that displacements associated with plastic design, can be computed manually and utilized advantageously without resorting to lengthy analysis or high power computers. The proposed methodologies offer displacement control options at first yield and incipient collapse. It has been shown that predetermined sequences of formation of plastic hinges could be arranged through rational selection of the strengths and stiffnesses of the constituent modules of the framework.

The advantage of the proposed concept over traditional methods of design is its ability to provide economic/optimized solutions while maintaining displacement control throughout the loading history of the moment frame.

In order to develop the proposed design concept for designing efficient moment frames without resorting to computers or complicated numerical analysis, recourse was been made to several axioms and structure specific principles, notably that: The full lateral load carrying and displacement development capacities of constitutive modules under combined gravity and lateral loading at incipient failure can be realized if the strength of the module is matched with the maximum static moments of its beams acting as simply supported elements. And, if the lateral performance of such modules can be enhanced by doubling the gravity capacity of their beams, then the performance of sub-frame as a whole can also be improved by doubling the plastic carrying capacities of its loaded beams.

The proposed procedures, as they stand are particularly useful for the preliminary design of short to midrise building structures.

REFERENCES

1. Beedle LS. *Plastic Design of Steel Frames.* John Wiley & Sons, 1958.
2. Baker JF, Horne MR, Hayman J. *The Steel Skeleton*, Cambridge University Press, Volumes 1-2, UK, 1956.
3. Neal BG. *The Plastic Methods of Structural Analysis*. Chapman & Hall Ltd. UK, 1963.
4. Nethercot DA. *Limit State Design of Structural Steelwork*, Spon Press, 2001.
5. NBCC National Building Code of Canada, National Research Council of Canada, Ottawa, 1995.
6. BS.5950, Davies JM, Brown B. Plastic Design to B.S. 5950, Steel Construction Institute, G. 1996.
7. AISC, (American Institute of Steel Construction) Seismic provisions for structural steel buildings, AISC, Chicago, Illinois, USA, 2005.
8. Mazzolani M, Piluso MV. Plastic design of seismic resistant steel frames, *Earthquake*

Eng Struct Dynam, 1997; **26**(2): 167–91.
9. Goel SC, Chao SH. Performance-based plastic design, ICC, 2008.
10. Wong MB. *Plastic Analysis and Design of Steel Structures*, Elsevier, 2009.
11. Grigorian M. An introduction to Performance control for moment frames of uniform response under lateral loading. *Asian J Civil Eng (BHRC)*, 2013; **14**(1): 123-43.
12. Naeim F. The Seismic Design Handbook, Kluwer Academic Publishers, 2001.
13. Bozorgnia Y, Bertero VV. Earthquake Engineering, CRC Press, 2004.
14. Priestly N, et. al. Displacement Based Seismic Design of Structures, IUSS Press, 2006.
15. Goel SC, Liao WC, Bayat MR, Chao SH. Performance-based plastic design (PBPD) method for earthquake resistant structures: An overview. *Struct Des Tall Spec Build*, 2010; **19**(1-2): 115–37.
16. Grigorian M, Grigorian C. Performance control for seismic design of moment frames, *J Construct Steel Res*, 2011; **67**: 1106-14.
17. Grigorian M. Grigorian C. Performance control: a new elastic-plastic design procedure for earthquake resisting moment frames. *J Struct Eng, ASCE,* 2012; **138**(6)**:** 473-83.
18. Dusenberry DO, Hamburger RO. Practical means for energy-based analyses of disproportionate collapse potential, *J Perform Constr Facil, ASCE* 2006 **20**(4), 336348.
19. Kim J, Park J. Design of moment Frames considering progressive collapse, *Steel composite Struct*, 2008; **8**(1): 85-98.
20. Kaveh A, Zolghadr A. Shape and size optimization of truss structures with frequency constraints using enhanced charged system search algorithm, *Asian J Civil Eng*, 2011; **12**(4): 487-509.
21. Kaveh A, Talatahari S. A novel heuristic optimization method: charged system search, *Acta Mech,* 2010; **213**(3-4): 267-89.
22. Kaveh A, Talatahari S. Charged System Search for Optimal Design of Planar Frame Structures, *Appl Soft Comput*, 2012; **12**(1): 382-93.
23. Kaveh A, Shahrouzi M. Simultaneous topology and size optimization of structures by genetic algorithm using minimal length chromosome, *Eng Comput*, 2006; **23**: 644-74.
24. Kaveh A, Farahmand Azar B, Hadidi A, Rezazadeh Sorochi F, Talatahari S. Performance-based seismic design of steel frames using ant colony optimization, *J Construct Steel Res*, 2010; **66**(4): 566-74.
25. Kaveh A, Khanlari K. Collapse load factor of planar frames using a modified Genetic algorithm, *Commun Numer Methods Eng*, 2004; **20**: 911-25.
26. Kaveh A, Talatahari S. An improved ant colony optimization for design of steel frames, *Eng Struct*, 2010; **32**: 864-73.
27. Kaveh A, Jahanshahi M. Plastic limit analysis of frames using ant colony systems, *Comput Struct*, 2008; **86**: 1152-63.
28. Kaveh A, Zakian P. Optimal design of steel frames under seismic loading using two meta-heuristic algorithms, *J Construct Steel Res*, 2013; **82**: 111-30.
29. Kaveh A, Mokhtar-Zadeh A. A combinatorial approach to optimal plastic design of structures, *Comput Mech*, Edit YK Cheung, JHW Lee, AYT Leung, AA Balkema / Rotterdam / Brookfield, 1991; **1**: 349-54.

30. Grigorian M, Grigorian C. An Introduction to the Methodology of Earthquake Resistant Structures of Uniform Response, *Buildings*, 2012; **2**: 107-25.
31. Grigorian M. On efficient design of earthquake resistant moment frames. *Asian J Civil Eng (BHRC)*, 2013; **14(2):** 319-38.
32. Brandt A. Criteria and Methods of Structural Optimization, Kluwer Academic publications, US. P.100, 1987.
33. Grigorian M. On the lateral response of regular high-rise frames, *Struct Des Tall Build*, 1993; **2**(3): 233–52.
34. Horne MR, Merchant W. *The Stability of Frames*, Pergamon Press, UK, 1965.
35. Hayman J, On the estimation of deflections in elastic plastic frames, *Proc. Inst. Civ. Eng.*, 1961; 19, 89.
36. Hayman J. *Plastic Design of Frames*, Cambridge University Press, UK, 1971.
37. Horne MR. *Plastic Theory of Structures*, Pergamon Press, (1979).
38. Grigorian M. Grigorian C. Lateral displacements of moment frames at incipient collapse, *Eng Struct*, 2012; **44**: 174–185
39. Grigorian M, Grigorian C. (1989) Preliminary minimum weight design of moment frames under lateral loading, *AISC Eng J*, 1st Quarter, 1989; **25**: 129-36.
40. Grigorian M, Grigorian C. A new performance based design approach for moment resisting frames, *Can J Civil Eng*, 2012; **39**:1–11.
41. Grigorian M, Grigorian C. Recent developments in plastic design analysis of steel moment frames, *J Construct Steel Res*, 2012; **76**: 83-92.
42. Hamburger RO, Krawinkler H, Malley JO, Adan SM. Seismic design of steel special moment frames: a guide for practicing engineers, *NEHRP Seismic Design Technical Brief*, Vol. 2, 2009.
43. Faulks J. Minimum weight design and the theory of plastic collapse. *Quart Appl Mech*, 1954; **10:** 347-59.
44. Faulks J. The minimum weight design of moment frames. *Proc Royal Society*, A.223, 1954; 482-494.
45. Heyman J. On the estimation of deflections in elastic plane structures. *Proc Inst Civil Engrs*, 1961; **19** : 39-60.
46. Heyman J, *Plastic Design of Frames*, Cambridge University Press, UK, 1973.

APPENDIX1: CASE 1, MODE III-3 DISPLACEMENT COMPUTATION

Let $\delta_{c,l}$ and $\delta_{c,r}$ represent the contributions of the left and right hand columns to the overall lateral displacement of the module. Next performing the virtual work summation using moment diagrams A1(a) and A1(c) it gives;

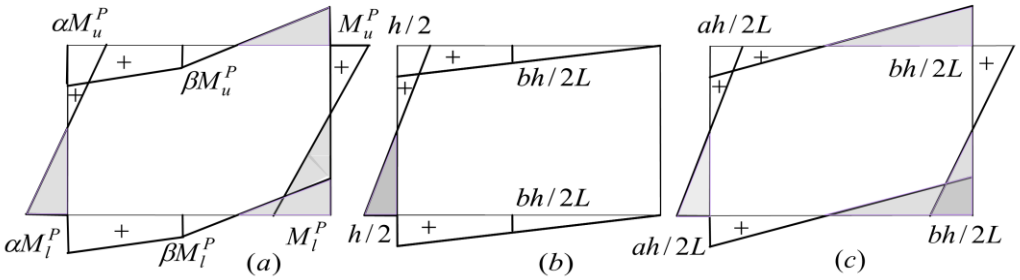

Figure A1. (a) generalized plastic moment distribution, (b) unit load moment diagram corresponding to $\beta<1$, (c) unit load moment diagram corresponding to $\beta=1$

$$\delta_{C,l}=\frac{h}{6EJ}\left[2\left(\alpha M_u^P\frac{ah}{2L}+\alpha M_l^P\frac{ah}{2L}\right)-\left(\alpha M_u^P\frac{ah}{2L}+\alpha M_l^P\frac{ah}{2L}\right)\right]=\frac{\alpha ah^2}{12EJL}\left(M_u^P+M_l^P\right) \tag{A1}$$

$$\delta_{C,r}=\frac{h}{6EJ}\left[2\left(M_u^P\frac{bh}{2L}+M_l^P\frac{bh}{2L}\right)-\left(M_u^P\frac{bh}{2l}+M_l^P\frac{bh}{2L}\right)\right]=\frac{bh^2}{12EJL}\left(M_u^P+M_l^P\right) \tag{A2}$$

$$\delta_C=\frac{h^2}{12EJL}\left(M_u^P+M_l^P\right)\left(\alpha a+b\right) \tag{A3}$$

Similarly if $\delta_{B,u}$ and $\delta_{B,u}$ represent the contributions of the upper and lower beams to the overall lateral displacement of the module, then performing the virtual work summation using moment diagrams 1g with and 1k it gives;

$$\delta_{B,u}=\frac{aM_u^P}{6EI_u}\left[2\left(\alpha\frac{ah}{2L}+0\right)+0+\beta\frac{ah}{2L}\right]+\frac{bM_u^P}{6EI_u}\left[2\left(0+\frac{bh}{2L}\right)+0-\beta\frac{bh}{2L}\right] \tag{A4}$$

$$\delta_{B,l}=\frac{aM_l^P}{6EI_l}\left[2\left(\alpha\frac{ah}{2L}+0\right)+0+\beta\frac{ah}{2L}\right]+\frac{bM_l^P}{6EI_l}\left[2\left(0+\frac{bh}{2L}\right)+0-\beta\frac{bh}{2L}\right] \tag{A5}$$

Next putting; $\beta=1$, in Eqs. (A4) and (A5), it gives,

$$\delta_B=\delta_{B,u}+\delta_{B,l}=\frac{h}{12EL}\left[(2\alpha+1)a^2+b^2\right]\times\left(\frac{M_u^P}{I_u}+\frac{M_l^P}{I_l}\right) \tag{A6}$$

The sum total of mathematical contributions of all four elements gives the maximum lateral displacement of the module at incipient collapse, thus;

$$\delta = \delta_C + \delta_B = \frac{h}{12EL}\left[\left(\frac{M_u^P + M_l^P}{J}\right)(\alpha a + b)h + \left(\frac{M_u^P}{I_u} + \frac{M_l^P}{I_l}\right)\left[(2\alpha + 1)a^2 + b^2\right]\right] \quad \text{(A7)}$$

APPENDIX2: CASE 2, MODE II DISPLACEMENT COMPUTATION

Let $\delta_{C,l}$ and $\delta_{C,r} = 0$ represent the contributions of the left and right hand columns to the overall lateral displacement of the module. Next performing the virtual work summation using moment diagrams A1(a) with $\alpha = 1$ and A1(b) it gives;

$$\delta_{C,l} = \frac{h}{6EJ}\left[2\left(M_u^P \frac{h}{2} + M_l^P \frac{h}{2}\right) - \left(M_u^P \frac{h}{2} + M_l^P \frac{h}{2}\right)\right] = \frac{h^2}{12EJ}\left(M_u^P + M_l^P\right) \quad \text{(A8)}$$

$$\delta_c = \frac{h^2}{12EJ}\left(M_u^P + M_l^P\right) \quad \text{(A9)}$$

Similarly if $\delta_{B,u}$ and $\delta_{B,u}$ represent the contributions of the upper and lower beams to the overall lateral displacement of the module, then performing the virtual work summation using the same moment diagrams, it gives;

$$\delta_{B,u} = \frac{bM_u^P}{6EI_u}\left[2\left(\beta\frac{bh}{2L} + \frac{h}{2}\right) + \frac{bh}{2L} + \beta\frac{h}{2}\right] + \frac{aM_u^P}{6EI_u}\left[2\left(0 + \beta\frac{bh}{2L}\right) + 0 - \frac{bh}{2L}\right] \quad \text{(A10)}$$

$$\delta_{B,l} = \frac{bM_l^P}{6EI_l}\left[2\left(\beta\frac{bh}{2L} + \frac{h}{2}\right) + \frac{bh}{2L} + \beta\frac{h}{2}\right] + \frac{aM_l^P}{6EI_l}\left[2\left(0 + \beta\frac{bh}{2L}\right) + 0 - \frac{bh}{2L}\right] \quad \text{(A11)}$$

$$\delta_B = \delta_{B,u} + \delta_{B,l} = \frac{h}{12E}\left\{b\left[\beta\left(\frac{2b}{L} + 1\right) + \left(2 + \frac{b}{L}\right)\right] + a\left[(2\beta - 1)\frac{b}{L}\right]\right\}\left[\frac{M_u^P}{I_u} + \frac{M_l^P}{I_l}\right] \quad \text{(A12)}$$

$$\delta = \delta_C + \delta_B =$$
$$\frac{h}{12E}\left\{\frac{h}{J}\left(M_u^P + M_l^P\right) + \left\{b\left[\beta\left(\frac{2b}{L} + 1\right) + \left(2 + \frac{b}{L}\right)\right] + a\left[(2\beta - 1)\frac{b}{L}\right]\right\}\left[\frac{M_u^P}{I_u} + \frac{M_l^P}{I_l}\right]\right\} \quad \text{(A13)}$$

APPENDIX3: MAXIMUM DISPLACEMENTS AT FIRST YIELD

The lateral displacements of the individual modules of Figure 3(c) can be expressed as;

$$\delta_j = \frac{V_j h^2}{24EI_j}\left(h + L_j\right) = \frac{V_j h^2}{24E} k_j = \frac{V_j}{K_{ji}} \quad \text{or} \quad \delta_s = \frac{V_s}{K_s} \tag{A14}$$

$$\text{Since } \delta_i = \delta = V / \sum_1^n K_j \text{ and } V = \sum_1^n V_j \text{ then } V_j = VK_j / \sum_1^n K_j \text{ and } V_s = VK_s / \sum_1^n K_j \tag{A15}$$

Now if $M_s = M_s^P$ then $V = V_Y$

$$\text{Therefore, } \left[\frac{K_j}{\sum_1^n K_j}\right] = \left[\frac{k_j}{\sum_1^2 k_{ji}}\right],\ M_s = M_s^P = \frac{V_Y h}{4}\left[\frac{K_s}{\sum_1^n K_j}\right] \text{ and } V_Y = \frac{4M_s^P}{h}\left[\frac{\sum_1^n K_j}{K_s}\right] \tag{A16}$$